

AFM investigation of silumin structure modified by Al-Y₂O₃ coating using the method of electric explosive alloying

K A Osintsev¹, K A Butakova¹, S V Konovalov², D V Zagulyaev¹
and V E Gromov¹

¹Siberian State Industrial University, 42 Kirova street, Novokuznetsk, 654007, Russia

²Samara National Research University, 34 Moskovskoye shosse, Samara, 443086, Russia

E-mail: zagulyaev_dv@physics.sibsiu.ru

Abstract The paper reports on coating of silumin samples with Al-Y₂O₃ by electric explosive alloying. When testing the micro-hardness, two appropriate processing modes of samples were revealed; the porosity of their surface profile was examined using atomic-force microscopy. A multi-layer structure was disclosed by metallographic microscopy, the thickness of each layer in the coating was determined as well. The mechanism of this structure formation was suggested.

1. Introduction

To date, silumins are broadly used in aircraft and ship construction, airspace industry and mechanical engineering but their insufficient strength properties and crack-resistance make them less utilized in comparison to more durable materials [1, 2].

The researchers [3-5] emphasize that the coating formation by electric explosive alloying makes it possible to enhance strength, durometric and tribological properties of the modified material. The strengthening effect is achieved due to the formation of coatings with fine-dispersed phases in the viscous metallic matrix [3].

The objective of this study is to investigate the effect of electric explosive alloying with a powder portion of Al-Y₂O₃ on the strength properties of silumin AK10M2H, as well as on the structure of its sub-surface layers.

2. Materials and methods

For the purpose of research the silumin samples AK10M2H were used; they were cut from one-piece bar, had a form of a parallelepiped with dimensions 20×20×10 mm³. Using electric explosive alloying the silumin substrate was coated with composites of the Al-Y₂O₃ system by the electric explosive unity EVU 60/10 (Siberian State Industrial University, Novokuznetsk). The electric explosive unit has the following parameters of alloying by plasma, which is formed in the electric explosion of aluminum foil with a powder portion of yttrium oxide: exposure time to plasma ~100 μs, absorbed power density on the jet axle ~8.2 GW/m², pressure in the shocked layer close to the surface ~18.8 MPa.

Front explosion was used [3-5] to intensify the heat impact on the material surface and further the melting process, providing conditions for alloying. The aluminium foil (0.0589 g) was hold between coaxial electrodes, which were supplied with adjustable voltage through a vacuum arrester. The



coatings were formed in thermal conditions, which lead to heating-up of the substrate surface up to the melting temperature at two different voltages: $U_1 = 2.6$ kV (samples 1, 3, 5) and $U_2 = 2.8$ kV (samples 2, 4, 6). Three samples with different weight of Y_2O_3 powder portion were used in each voltage mode. A powder portion of 0.0589 g was used for samples 1, 2; 0.02945 g – for samples 3, 4, and 0.0883 g – for samples 5, 6, respectively.

When discharging the capacitive energy storage, a periphery of the foil close to the outer electrode-nozzle is a source of a condensed phase of explosion products; a foil above the central electrode, where the powder of yttrium oxide is supplied, is a source of ionized vapour [4].

Completing the electric explosive alloying, Vickers micro-hardness tests were carried out (micro-hardness measuring device HVS-1000A). A load of 0.05 HV was constant for all six samples. The micro-hardness was measured in grains and eutectic.

The porosity of the coating and the heat-affected zone was investigated using an atomic-force microscope NT-MDT Solver “NEXT”, since it has high-performance and helps to carry out up to date procedures of research into the morphology and local properties of the solid surface with a high space resolution [6-8]. The topography of the surface profile was imaged.

The structure of the material was explored using a metallographic microscope Olympus GX-51. The images for measuring surface layer thicknesses were taken; a form and sizes of grains were analyzed, and the conclusion on uniformity of the formed coating was drawn.

3. Experiment results

In accordance with the experimental measurements of micro-hardness (table 1) the correlation of micro-hardness to the distance of the coated layer (coating included) was plotted (figure 1). From the statistical data of the experiment the maximal micro-hardness of samples 2 and 5 is apparent. A significant increase in the micro-hardness is disclosed in these samples close to the surface, both in grains and in eutectic. The micro-hardness of the surface in samples 2 and 5 is higher than samples, in total, by 50 % and 65 %, respectively.

Table 1. Micro-hardness test results of silumin samples subjected to electric explosive alloying with $Al-Y_2O_3$.

Sample No.	Phase	520 μ m from the edge	90 μ m from the edge	70 μ m from the edge	50 μ m from the edge	Composite surface layer
1	Grain	54	56.03	51.16	78.48	78.55
	Eutectic	67.04	66.15	72.73	94.17	
2	Grain	63	59.36	63.92	87	130.51
	Eutectic	73.99	89.5	89.22	87.92	
3	Grain	58.67	58.55	57.53	61.64	57.12
	Eutectic	79.96	76.18	74.78	84.15	
4	Grain	59.53	58	67.88	73.34	77.34
	Eutectic	80.37	72.76	80.62	85.65	
5	Grain	63.09	65.61	67.58	66.58	161.2
	Eutectic	108.7	105.17	122.34	111.57	
6	Grain	86.56	66.84	77	81.31	101.56
	Eutectic	88.31	94.56	86.49	103.51	

From the curves (figure 1) it can be seen that the micro-hardness both in grains and eutectic of the modified samples increases close to the coated layer.

The metallographic study on the cross-section structure of the samples with the maximal micro-hardness (samples 2 and 5) revealed a multi-layered structure consisting of a highly-porous coating with non-uniform thickness, a layer of liquid-phase alloying, and a heat-affected layer c (figure 2 a, b). The thickness of the modified layer ranges from 17 to 117 μm for sample 2 and from 33 to 60 μm for sample 5 owing to the precisely determined weight of the coated powder – less Y_2O_3 was used for sample 2 than for sample 5. Therefore, the coating of sample 5 was more uniform in the width than of sample 2. The thickness of the heat-affected layer is 150–260 μm in sample 2 and 53–80 μm in sample 5, respectively. The heat-affected layer in sample 2 is significantly thicker than in sample 5 due to higher energy mode of coating for sample 2.

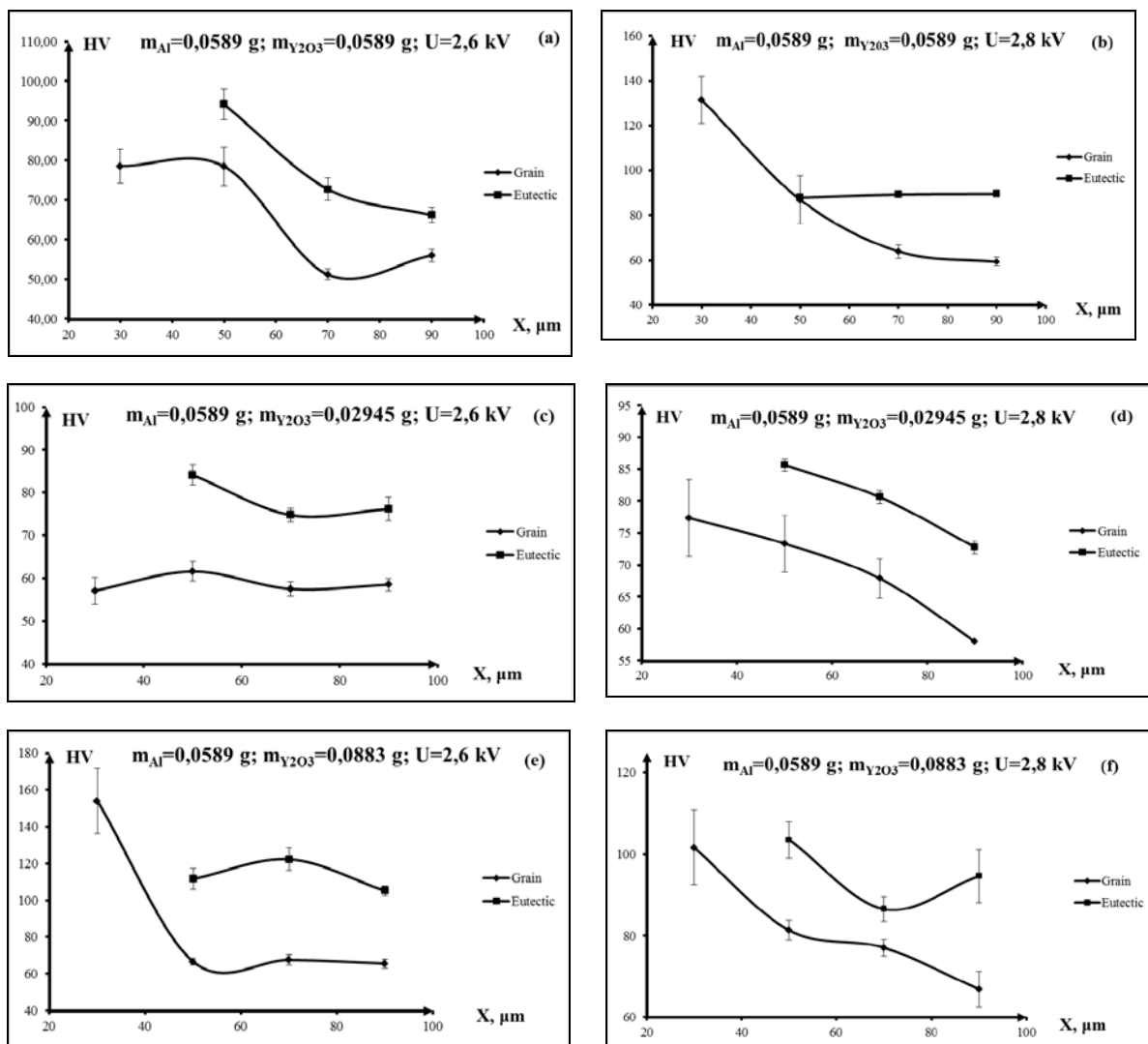


Figure 1. Micro-hardness in grains and eutectic of silumin samples in different processing modes vs. distance to the sample surface.

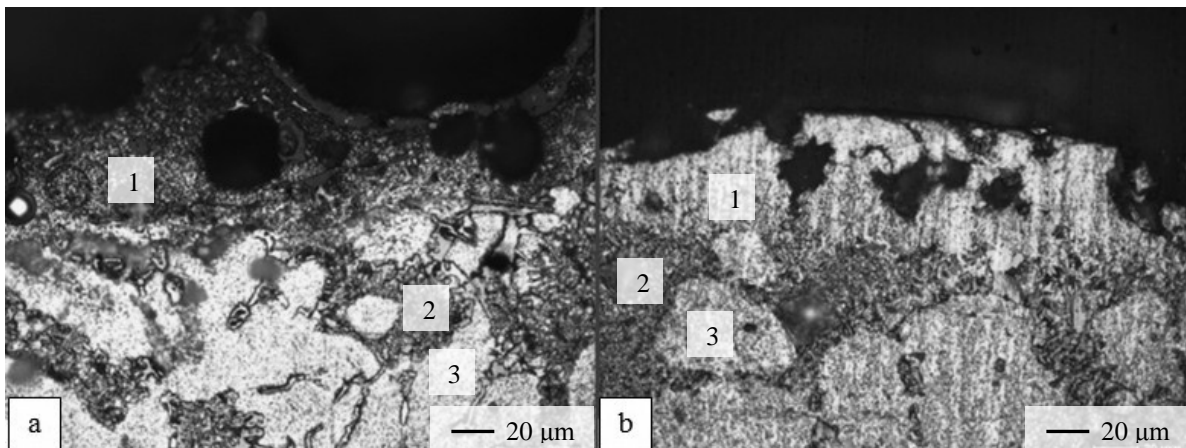


Figure 2. Optical microscopy of the surface profile in silumin samples processed in modes 2 (a) and 5 (b): 1 – modified layers, 2 – eutectic, 3 – grains.

The topography of the surface profiles imaged by atomic-force microscopy is shown in figures 3 – 6. 3D and 2D images, as well as asperity profiles along the base line in the sample (coating excluded) and on the coatings are presented.

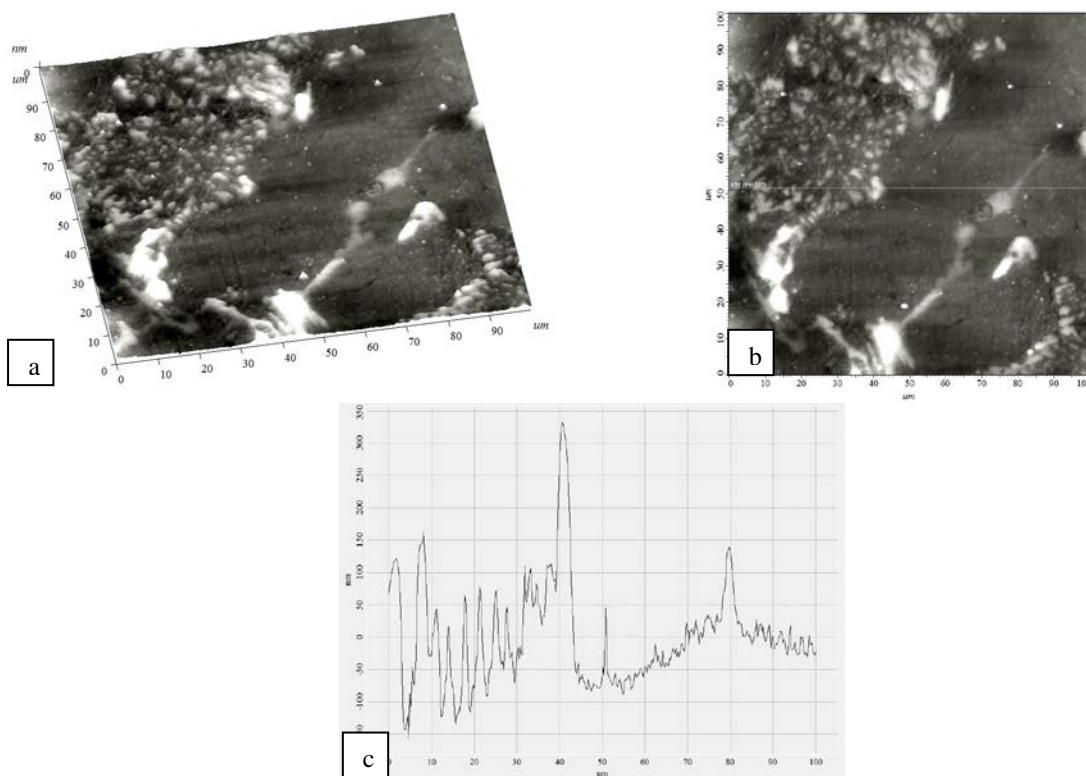


Figure 3. Atomic-force microscopy of the surface profile in sample 2 (coating excluded): a – profile asperity according to the height in 3D, b – 2D image of the surface profile topography with a drawn section, c – asperity distribution along the base length.

The structure of the modified silumin in the sample (coating excluded) comprises grains with a height of 350 nm and relatively smooth eutectic.

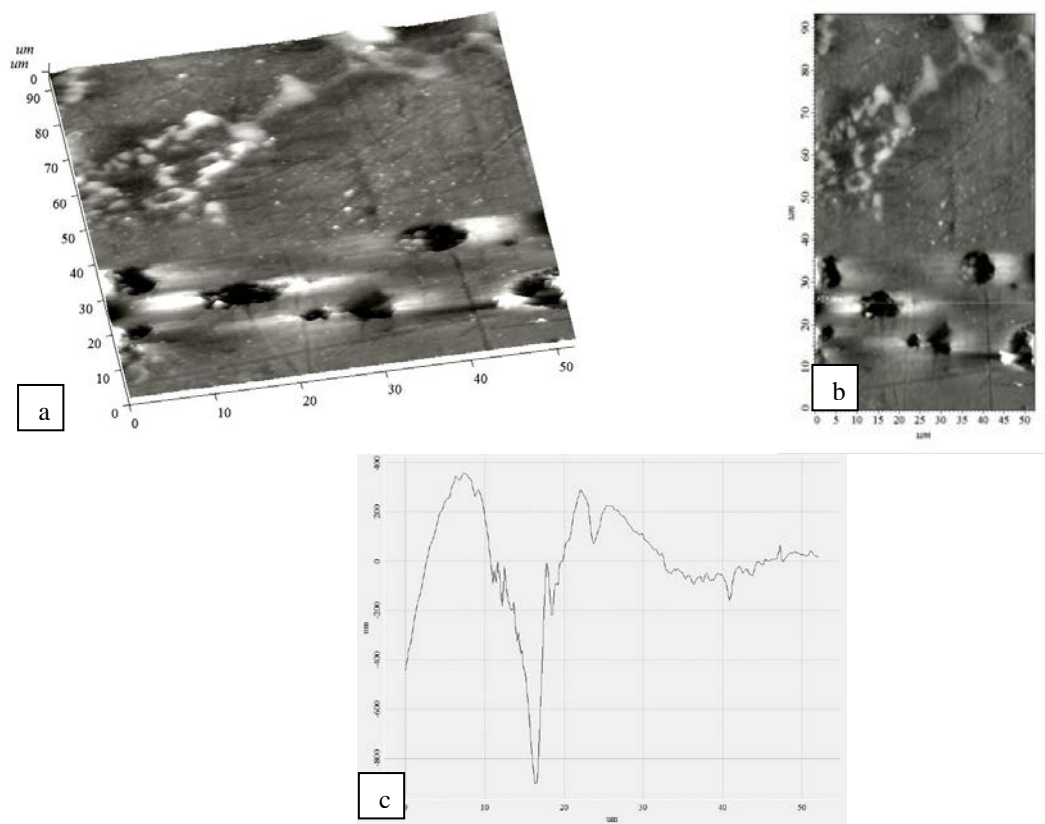
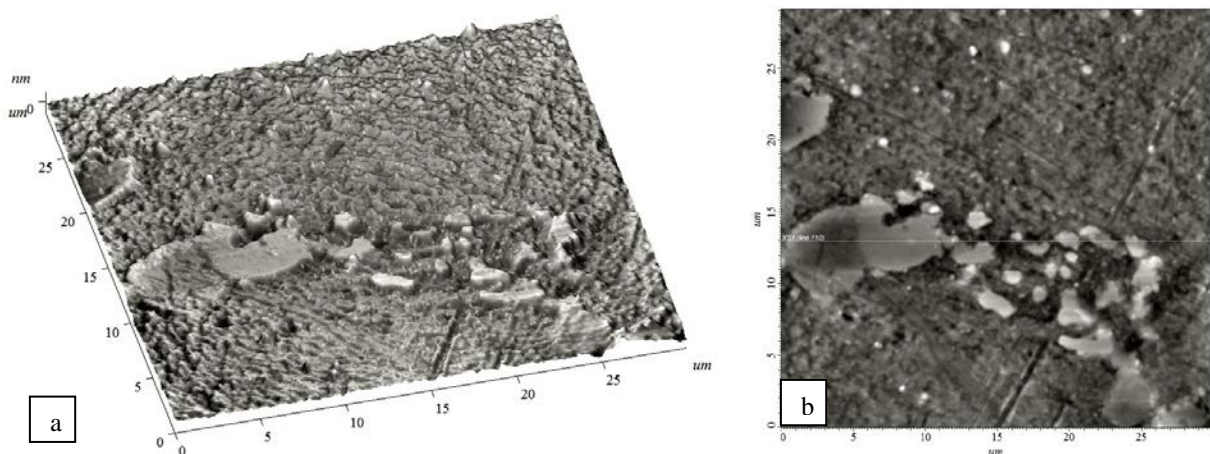


Figure 4. Atomic-force microscopy of the surface profile in the coated layer of sample 2: a – profile asperity according to the height in 3D, b – 2D image of the surface profile topography with a drawn section, c – asperity distribution along the base length.

As seen in figure 4, the coating in sample 2 is a highly-porous one. Statistical processing of images revealed a maximum depth of pores (1500 nm). The diameter of pores is up to 10 μm .



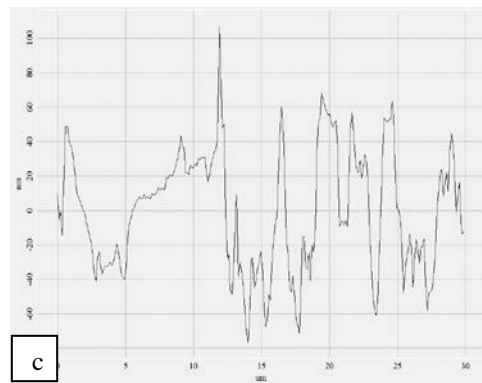


Figure 5. Atomic-force microscopy of the surface profile in sample 2 (coating excluded): a – profile asperity according to the height in 3D, b – 2D image of the surface profile topography with a drawn section, c – asperity distribution along the base length.

Sample 5 (coating excluded) similar to sample 2 (coating excluded) has a structure comprising eutectic and grains.

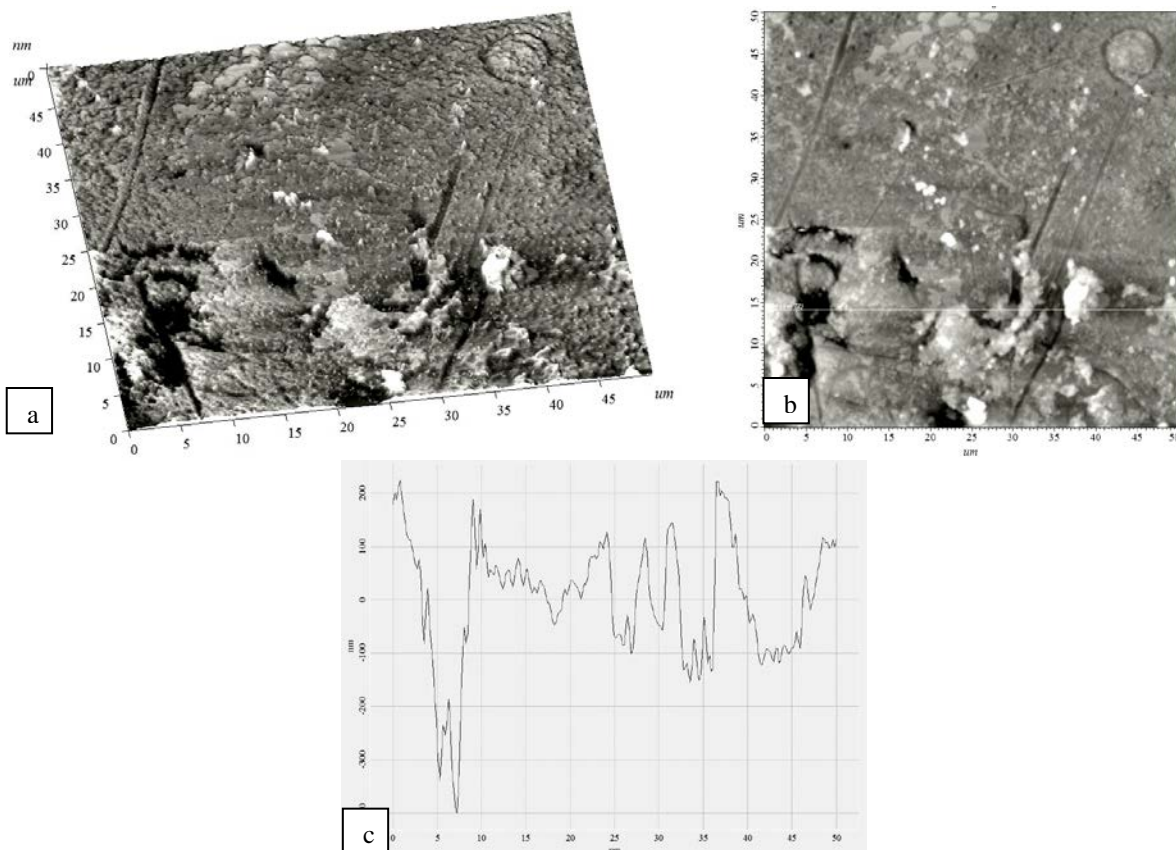


Figure 6. Atomic-force microscopy of the coated layer surface profile of sample 5: a – profile asperity according to the height in 3D, b – 2D image of the surface profile topography with a drawn section, c – asperity distribution along the base length.

From figure 6 it is apparent that the coating in sample 5 is porous. The number and depth of pores are less significant than in the coated layer in sample 2. The maximal depth of pores is 500 nm. The explanation is that owing to higher weight of a portion of the sprayed powder and lower energy impact, particles of a plasma jet with lower energy are distributed more uniformly. Kelvin–Helmholtz instability is possible as well, i.e. remixing of coated and melted layers; as a consequence, there are fewer pores than in sample 2.

4. Conclusion

In the course of the work, it is found that electric explosive alloying leads to the increase in microhardness in the silumin surface layer and optimal treatment regimes are determined, in which the microhardness value increases by 50-65%.

Study of the structure of silumin surface profile by metallographic and atomic force microscopy shows that thanks to electric explosive alloying a multilayer structure is formed, which consists of a highly porous coating, non-uniform in thickness, a layer of liquid-phase alloying and a layer of thermal influence.

An assumption is put forward that the formation mechanism of the resulting structure is the flow of Kelvin-Helmholtz instability, i.e. the mixing of the sprayed and melted layers, resulting in a reduced number of pores.

Acknowledgements

This work was supported by the State Order 3.1283.2017/4.6.

References

- [1] Martyushev N V, Bashev V S and Zykova A P 2017 *IOP Conf. Ser.: Mater. Sci. Eng.* **177** 012118
- [2] Konovalov S V, Alsaraeva K V, Gromov V E and Ivanov Yu F 2015 *IOP Conf. Ser.: Mater. Sci. Eng.* **91** 012029
- [3] Vashchuk E S, Romanov D A, Budovskikh E A and Ivanov Y F 2011 *Steel in Transl.* **41** (6) 469–474
- [4] Romanov D A, Budovskikh E A and Gromov V E 2011 *J. Of Surf. Invest.: X-Ray, Synch. And Neutr. Tech.* **5** (6) 1112–17
- [5] Ivanov Y F, Budovskikh E A, Gromov V E, Bashchenko L P, Soskova N A and Raikov S V 2012 *Steel in Transl* **42** (6) 499–501
- [6] Haviland D B 2017 *Current Op. in Coll. & Int. Sci.* **27** 74–81
- [7] Yuan Li and Cheng Y F 2016 *App. Surf. Sci.* **366** 96–103
- [8] Lee S W 2016 *Synt. Met.* **216** 88–92
- [9] Sarychev V D, Vashchuk E S Budovskikh E A and Gromov V E 2010 *Tech. Phys.* **36(7)** 656–659
- [10] Granovskii A Y, Sarychev V D and Gromov V E 2013 *Tech. Phys.* **58(10)** 1544–47